



# *Streptococcus pneumoniae*, *S. mitis*, and *S. oralis* Produce a Phosphatidylglycerol-Dependent, *ItaS*-Independent Glycerophosphate-Linked Glycolipid

Yahan Wei,<sup>a</sup> Luke R. Joyce,<sup>a</sup> Ashley M. Wall,<sup>a</sup> Ziqiang Guan,<sup>b</sup> Kelli L. Palmer<sup>a</sup>

<sup>a</sup>Department of Biological Sciences, The University of Texas at Dallas, Richardson, Texas, USA

<sup>b</sup>Department of Biochemistry, Duke University Medical Center, Durham, North Carolina, USA

**ABSTRACT** Lipoteichoic acid (LTA) is a Gram-positive bacterial cell surface polymer that participates in host-microbe interactions. It was previously reported that the major human pathogen *Streptococcus pneumoniae* and the closely related oral commensals *S. mitis* and *S. oralis* produce type IV LTAs. Herein, using liquid chromatography/mass spectrometry-based lipidomic analysis, we found that in addition to type IV LTA biosynthetic precursors, *S. mitis*, *S. oralis*, and *S. pneumoniae* also produce glycerophosphate (Gro-P)-linked dihexosyl (DH)-diacylglycerol (DAG), which is a biosynthetic precursor of type I LTA. *cdsA* and *pgsA* mutants produce DHDAG but lack (Gro-P)-DHDAG, indicating that the Gro-P moiety is derived from phosphatidylglycerol (PG), whose biosynthesis requires these genes. *S. mitis*, but not *S. pneumoniae* or *S. oralis*, encodes an ortholog of the PG-dependent type I LTA synthase, *ItaS*. By heterologous expression analyses, we confirmed that *S. mitis* *ItaS* confers poly(Gro-P) synthesis in both *Escherichia coli* and *Staphylococcus aureus* and that *S. mitis* *ItaS* can rescue the growth defect of an *S. aureus* *ItaS* mutant. However, we do not detect a poly(Gro-P) polymer in *S. mitis* using an anti-type I LTA antibody. Moreover, Gro-P-linked DHDAG is still synthesized by an *S. mitis* *ItaS* mutant, demonstrating that *S. mitis* *ItaS* does not catalyze Gro-P transfer to DHDAG. Finally, an *S. mitis* *ItaS* mutant has increased sensitivity to human serum, demonstrating that *ItaS* confers a beneficial but currently undefined function in *S. mitis*. Overall, our results demonstrate that *S. mitis*, *S. pneumoniae*, and *S. oralis* produce a Gro-P-linked glycolipid via a PG-dependent, *ItaS*-independent mechanism.

**IMPORTANCE** The cell wall is a critical structural component of bacterial cells that confers important physiological functions. For pathogens, it is a site of host-pathogen interactions. In this work, we analyze the glycolipids synthesized by the mitis group streptococcal species, *S. pneumoniae*, *S. oralis*, and *S. mitis*. We find that all produce the glycolipid, glycerophosphate (Gro-P)-linked dihexosyl (DH)-diacylglycerol (DAG), which is a precursor for the cell wall polymer type I lipoteichoic acid in other bacteria. We investigate whether the known enzyme for type I LTA synthesis, *ItaS*, plays a role in synthesizing this molecule in *S. mitis*. Our results indicate that a novel mechanism is responsible. Our results are significant because they identify a novel feature of *S. pneumoniae*, *S. oralis*, and *S. mitis* glycolipid biology.

**KEYWORDS** *ItaS*, *Streptococcus mitis*, *Streptococcus oralis*, *Streptococcus pneumoniae*, glycolipids, lipidomics, lipoteichoic acid

The Gram-positive bacteria *Streptococcus mitis* and *S. oralis*, members of the mitis group streptococci, are among the major oral colonizers that protect against human gingivitis via production of hydrogen peroxide, neutralization of acids, and secretion of antimicrobial compounds (1–5). They are also opportunistic pathogens

**Citation** Wei Y, Joyce LR, Wall AM, Guan Z, Palmer KL. 2021. *Streptococcus pneumoniae*, *S. mitis*, and *S. oralis* produce a phosphatidylglycerol-dependent, *ItaS*-independent glycerophosphate-linked glycolipid. *mSphere* 6:e01099-20. <https://doi.org/10.1128/mSphere.01099-20>.

**Editor** Craig D. Ellermeier, University of Iowa

**Copyright** © 2021 Wei et al. This is an open-access article distributed under the terms of the [Creative Commons Attribution 4.0 International license](https://creativecommons.org/licenses/by/4.0/).

Address correspondence to Ziqiang Guan, [ziqiang.guan@duke.edu](mailto:ziqiang.guan@duke.edu), or Kelli L. Palmer, [Kelli.L.Palmer@utdallas.edu](mailto:Kelli.Palmer@utdallas.edu).

**Received** 27 October 2020

**Accepted** 5 February 2021

**Published** 24 February 2021

that are among the leading causes of community-acquired bacteremia and infective endocarditis (IE) (6–8). Our understanding of how these organisms colonize, survive, and interact with the human host in these different niches is incomplete and requires further mechanistic study.

*Streptococcus pneumoniae* also belongs to the mitis group streptococci and shares >99% identity in 16S rRNA sequence with both *S. mitis* and *S. oralis* (9, 10). *S. pneumoniae* mainly colonizes the mucosal surfaces of the human upper respiratory tract and is a well-known human pathogen causing pneumonia, meningitis, and otitis media, among other infections, and is a significant cause of morbidity and mortality worldwide (11, 12). Though *S. mitis*, *S. oralis*, and *S. pneumoniae* differ in their colonization abilities and pathogenic potential, multiple studies have shown that they share some common mechanisms of host-microbe interactions. For instance, *S. mitis* and *S. oralis* may serve as reservoirs of pneumococcal virulence-associated and antibiotic resistance genes (13–15), and immunity against *S. mitis* provides protection against *S. pneumoniae* colonization (16). We recently reported that *S. mitis*, *S. oralis*, and *S. pneumoniae* scavenge intermediates of human phospholipid metabolism and utilize them to synthesize the zwitterionic phospholipid phosphatidylcholine (PC), a pathway that potentially modulates human host immune responses (17, 18).

In addition to membrane phospholipids, another Gram-positive cell wall component that plays critical roles in host-microbe interactions is the lipoteichoic acid (LTA). Teichoic acid (TA) is a polymer typically consisting of either glycerophosphate (Gro-P) or ribitol-phosphate (Rbo-P) repeating units (19). Depending on its cell surface anchor, the TA polymer is either called wall teichoic acid (WTA), which is anchored to the peptidoglycan layers, or LTA, which is anchored to membrane lipids. LTAs with different chemical structures can trigger different immune responses from the host (20–22). According to their structural differences, LTAs have been grouped into five different types, among which the LTAs produced by *Staphylococcus aureus* (type I) and *S. pneumoniae* (type IV) have been extensively studied (23). Pneumococcal LTA was originally identified in 1943, and it was named F-antigen at that time due to its ability to cross-react with the Forssman antigen series (24). Its repeating unit consists of residues of 2-acetamido-4-amino-2,4,6-trideoxy-D-galactose (AATGal), D-glucose, Rbo-P, N-acetyl-D-galactosamine (GalNAc), and phosphocholine (25). Genes involved in the production of type IV LTA were summarized by Denapaita et al. based on genomic predictions and previous experimental studies (26). Orthologs of these genes are also present in *S. oralis* and *S. mitis* genomes, except that for most *S. mitis* and *S. oralis* strains, the glucose glycosyltransferase is substituted with a galactose glycosyltransferase (26, 27). Structural analysis of the type IV LTA produced by *S. oralis* strain Uo5 has confirmed the replacement of glucose residues by galactose, as well as revealed other differences relative to pneumococcal LTA in the repeating unit and branching structures (28).

*S. mitis* is the primary focus of the work presented here. In *S. mitis*, differently structured LTA-like polymers have been reported. Previously, Bergström et al. found that 39 of 77 *S. mitis* strains produce polysaccharide polymers detectable by monoclonal antibodies that separately target the pneumococcal type IV LTA polymer backbone and phosphocholine residues (29). Among the remaining strains, some of them lack phosphocholine, such as *S. mitis* SK598, which produces a pneumococcal LTA-like polymer with the choline residues being replaced by ethanolamine (29, 30). In addition, a few studies have reported detection of type I-like LTA, a Gro-P polymer, from *S. mitis* clinical isolates using anti-type I LTA antibodies (31–33). However, since these reports, species definitions among mitis group streptococci have been refined. A more recent reanalysis using the same detection technique did not detect type I LTA in four *S. mitis* strains, including the type strain *S. mitis* ATCC 49456 (34). However, genomic analysis supports the possibility of type I LTA synthesis in *S. mitis*, as *S. mitis* encodes an ortholog of the *S. aureus* type I LTA synthase gene, *ltaS* (26, 35). *ltaS* catalyzes the transfer of Gro-P from the membrane phospholipid phosphatidylglycerol (PG) and polymerizes the Gro-P units on a glycolipid anchor, forming type I LTA (36, 37).

The goal of our study was to determine whether *S. mitis* produces multiple types of LTAs and whether *S. mitis ltaS* mediates production of type I LTA, using the type strain ATCC 49456 as a model. We used normal-phase liquid chromatography (NPLC)-electrospray ionization/mass spectrometry (ESI/MS) to analyze membrane lipids in the mitis group streptococci. This technique is highly sensitive and specific and allows for the detection and characterization of LTA anchors and other LTA biosynthetic intermediates whose cellular levels are too low to be detected by conventional techniques such as thin-layer chromatography (TLC). We identified intermediates of type IV LTA synthesis in *S. mitis*, *S. oralis*, and *S. pneumoniae*. To our surprise, a type I-like LTA intermediate was observed not only in *S. mitis*, which encodes *ltaS*, but also in *S. oralis* and *S. pneumoniae*, which lack *ltaS* orthologs. Moreover, while *S. mitis* ATCC 49456 *ltaS* confers poly(Gro-P) synthesis when heterologously expressed in *Escherichia coli* and an *S. aureus ltaS*-deficient mutant, we confirm that *S. mitis* ATCC 49456 does not produce a polymer detectable by a type I LTA antibody. Importantly, *ltaS* contributes to *S. mitis* ATCC 49456 fitness, because deletion of *ltaS* impacted growth in human serum-supplemented medium. Overall, our results demonstrate that *S. mitis*, *S. oralis*, and *S. pneumoniae* synthesize intermediates of two structurally distinct lipid-anchored polymers, one type IV LTA, and one a Gro-P-containing polymer whose full structure remains to be determined.

## RESULTS

**Mitis group streptococci produce glycolipid intermediates of two structurally distinct LTAs.** LTA is usually anchored to the membrane by a saccharide-linked diacylglycerol (DAG) glycolipid (23). Structure of the glycolipid anchor varies among different LTA types, bacterial species, and even culture conditions (38). In *S. pneumoniae*, the pseudopentasaccharide repeating units of type IV LTA are proposed to be assembled on an undecaprenyl pyrophosphate ( $C_{55}$ -PP) anchor and then transferred to a glucosyl-DAG (Glc-DAG) anchor (Fig. 1A) (25). In *S. aureus*, type I LTA is typically assembled on a diglucosyl-DAG (Glc<sub>2</sub>-DAG) anchor (Fig. 1A) (39). *Listeria monocytogenes* also produces type I LTA, which is linked to a galactosyl-glucosyl-DAG (Gal-Glc-DAG) anchor (40). Thus, lipid profiling has the potential to identify LTA intermediates, thereby revealing possible types of LTAs produced by a bacterium. To perform lipidomic analysis of mitis group streptococci, total lipids were extracted from bacterial cultures with a modified acidic Bligh-Dyer method and analyzed with NPLC-ESI/MS (41). We analyzed the type strain of *S. mitis* (ATCC 49456, referred to as SM61 hereafter), *S. oralis* (ATCC 35037 and the endocarditis isolate 1647), two clinically isolated *S. pneumoniae* strains (D39 and TIGR4), and *Streptococcus* sp. strain 1643 (referred to as SM43 hereafter), a human endocarditis isolate that was clinically identified as *S. mitis* but shares higher genomic identity with *S. oralis* (Table 1) (18, 42).

Three  $C_{55}$ -PP-linked intermediates of type IV LTA biosynthesis were detected in all strains analyzed. Specifically, these intermediates are  $C_{55}$ -PP-linked AATGal ( $[M-H]^-$  at  $m/z$  1111.7 of Fig. 1B, left),  $C_{55}$ -PP-AATGal-Gal ( $[M-H]^-$  at  $m/z$  1273.7 of Fig. 1B, middle, and see Fig. S1, bottom, in the supplemental material), and  $C_{55}$ -PP-AATGal-Gal-(Rbo-P) ( $[M-H]^-$  at  $m/z$  1487.7 of Fig. 1B, right). Identifications of these species are supported by the exact mass measurement and tandem mass spectrometry (MS/MS). For example, Fig. 1C shows MS/MS of the doubly deprotonated  $[M-2H]^{2-}$  ion at  $m/z$  743.4 for  $C_{55}$ -PP-AATGal-Gal-(Rbo-P) along with the fragmentation scheme. In addition, we also detected (Gro-P)-dihexosyl (DH)-DAG ( $[M-H]^-$  at  $m/z$  1071.6 of Fig. 1D and Fig. S2), an intermediate that would be expected for type I LTA. The exact mass measurement ( $m/z$  1071.620) is consistent with the calculated  $[M-H]^-$  ion mass ( $m/z$  1071.624) of (Gro-P)-DHDAG containing  $C_{16:0}$  and  $C_{18:1}$  acyl chains. Furthermore, MS/MS of  $[M-H]^-$  ion at  $m/z$  1071.6 for (Gro-P)-DHDAG (16:0/18:1) along with the fragmentation scheme are shown in Fig. 1D. The stereochemistry of the two hexoses cannot be discerned by MS/MS.

To confirm the possible monosaccharide identity of the DAG-linked sugars, *in silico* analyses were performed to identify orthologs of known glycolipid biosynthetic genes in the genomes of the tested strains. *S. pneumoniae* produces the glycolipid Gal-Glc-

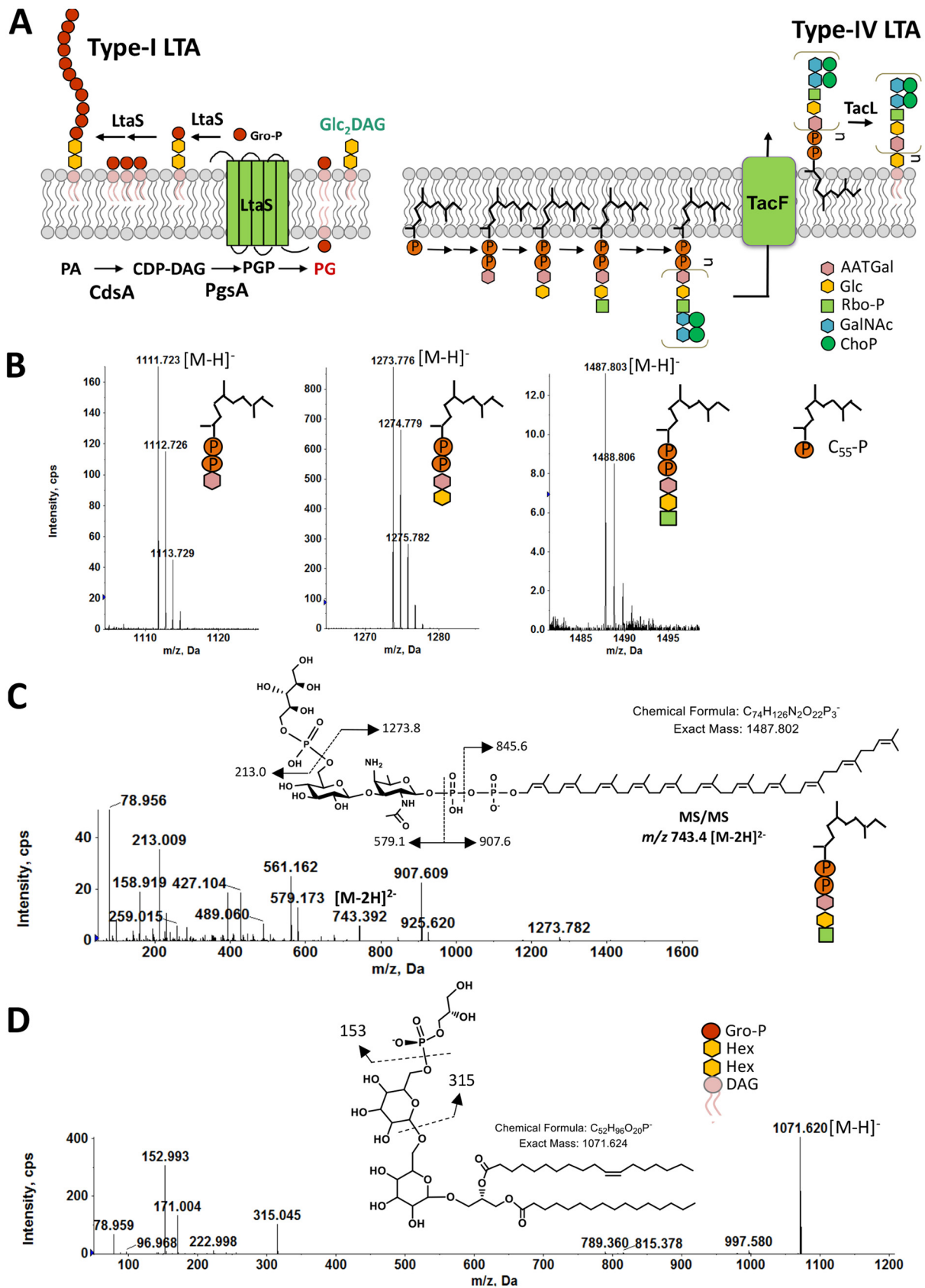


**FIG 1** Detection of type IV LTA biosynthetic precursors and (Gro-P)-dihexosyl-DAG from the lipid extracts of *S. mitis* ATCC 49456 (SM61). Total lipids were extracted from *S. mitis* grown to mid-log phase in Todd-Hewitt broth. (A) Schematic of biosynthesis of *S. aureus* type I and (Continued on next page)

**TABLE 1** Detection of lipoteichoic acid intermediates from selected strains of mitis group streptococci

Bacterial species	Strain	Presence of biosynthetic precursor		
		(Gro-P)-dihexosyl-DAG <sup>a</sup>	Dihexosyl-DAG	AATGal-Gal-(Rbo-P) <sup>b</sup>
<i>S. mitis</i> ATCC 49456 (SM61)	WT <sup>c</sup>	Yes	Yes	Yes
	$\Delta cdsA$	<b>No</b>	Yes	Yes
	$\Delta ItaS$	Yes	Yes	Yes
<i>Streptococcus</i> sp. 1643 (SM43)	WT	Yes	Yes	Yes
	$\Delta cdsA$	<b>No</b>	Yes	Yes
	$\Delta pgsA$	<b>No</b>	Yes	Yes
<i>S. oralis</i> ATCC 35037	WT	Yes	Yes	Yes
<i>S. oralis</i> 1647	WT	Yes	Yes	Yes
<i>S. pneumoniae</i>	D39	Yes	Yes	Yes
	TIGR4	Yes	Yes	Yes

<sup>a</sup>The absence of a biosynthetic precursor is indicated by a bold italic No for emphasis.

<sup>b</sup>AATGal-Glc-(Rbo-P) in *S. pneumoniae*.

<sup>c</sup>WT, wild type.

DAG (43), for which the biosynthetic genes have been partially identified. These genes can be separated into two major groups corresponding to the biosynthetic steps they are responsible for: (i) production of nucleotide-activated sugars and (ii) transferring of the activated sugar moieties to DAG (38). As shown in Table 2, these genes include the following: confirmed UDP glucose (UDP-Glc) production gene *pgm* (encoding  $\alpha$ -phosphoglucomutase) and *galU* (encoding UTP: $\alpha$ -glucose-1-phosphate uridylyltransferase) (44); Leloir pathway genes that are proposed to produce UDP galactose (UDP-Gal), specifically *galK* (encoding galactokinase) and *galT2* (encoding galactose-1-phosphate uridylyltransferase 2) (45, 46); and glycosyltransferases encoded by genes Spr0982 and *cpoA* which sequentially transfer Glc and Gal residues to DAG, respectively (47, 48). *S. pneumoniae* R6 is an avirulent and unencapsulated derivative of *S. pneumoniae* D39 (49). These two strains share the same glycolipid biosynthetic genes. Using *S. pneumoniae* R6 as reference, orthologs of Gal-Glc-DAG biosynthetic genes with  $\geq 87\%$  amino acid identity were identified in the genomes of SM61, *S. oralis* ATCC 35037, SM43, and *S. pneumoniae* TIGR4 (Table 2). This analysis suggests that the DHDAG detected in our experiments is likely to be Gal-Glc-DAG.

**Biosynthesis of (Gro-P)-DHDAG requires phosphatidylglycerol in mitis group streptococci.** In *S. aureus*, the Gro-P of type I LTA is produced from hydrolyzation of membrane PG (36), a process that is also required for Gro-P modification of streptococcal rhamnose-containing cell wall polysaccharides (50). To verify whether PG is the source of Gro-P for (Gro-P)-DHDAG biosynthesis in mitis group streptococci, we analyzed the lipid profiles of *cdsA* and *pgsA* mutants. The gene *cdsA* is required for the synthesis of CDP-DAG, which is then converted by PgsA to produce phosphatidylglycerophosphate (PGP), the immediate precursor of PG (Fig. 1A) (18, 41). We previously reported that *cdsA* deletion mutants of *S. mitis* and *S. oralis* do not synthesize PG, nor does a *pgsA* deletion mutant of SM43 (18, 41) (Fig. 2). Thus, lipid anchor profiles of

#### FIG 1 Legend (Continued)

*S. pneumoniae* type IV LTAs. (B) Negative ion ESI mass spectra showing the  $[M-H]^-$  ions of  $C_{55}$ -PP-AATGal,  $C_{55}$ -PP-AATGal-Gal, and  $C_{55}$ -PP-AATGal-Gal-(Rbo-P). These  $C_{55}$ -PP-linked saccharides are intermediates involved in assembling the pseudopentasaccharide repeating units of type IV LTA. Intensity is shown in copies per second (cps). (C) MS/MS product ion mass spectrum of the  $m/z$  743.4  $[M-2H]^{2-}$  ion of  $C_{55}$ -PP-AATGal-Gal-(Rbo-P) and the MS/MS fragmentation scheme. (D) MS/MS of the  $m/z$  1071.6  $[M-H]^-$  ion of (Gro-P)-dihexosyl-DAG and the proposed fragmentation scheme. The chemical structures presented in panels C and D are for illustrative purposes only. The stereochemistry and linkage of hexose moieties, as well as the phosphate position on the glycerol, could not be determined by tandem MS. Abbreviations: PA, phosphatidic acid; CDP, cytidine diphosphate; PG, phosphatidylglycerol; PGP, PG-3-phosphate; Glc, glucose;  $C_{55}$ -PP, undecaprenyl pyrophosphate; DAG, diacylglycerol; Gal, galactosyl; Gro-P, glycerophosphate; Rbo-P, ribitol-phosphate; AATGal, 2-acetamido-4-amino-2,4,6-trideoxy-D-galactose; GalNAc, N-acetyl-D-galactosamine; ChoP, phosphocholine; Hex, hexose.

**TABLE 2** Orthologs of glycolipid biosynthetic genes

Chemical precursor <sup>a</sup>	Biosynthetic enzyme (reference gene <sup>b</sup> )	<i>S. mitis</i> ATCC 49456		<i>S. oralis</i> ATCC 35037		<i>Streptococcus</i> sp. 1643		<i>S. pneumoniae</i> TIGR4	
		Locus tag	AA <sup>c</sup>	Locus tag	AA	Locus tag	AA	Locus tag	AA
UDP-Glc	$\alpha$ -Phosphoglucomutase ( <i>pgm</i> ) (44)	SM12261_RS05265	98.6	HMPREF8579_1344	97.0	FD735_RS05500	97.2	SP_1498	100.0
	UTP: $\alpha$ -glucose-1-phosphate uridylyltransferase ( <i>galU</i> ) (44)	SM12261_RS05330	95.3	HMPREF8579_0527	93.7	FD735_RS00655	93.7	SP_2092	95.7
UDP-Gal	Galactokinase ( <i>galk</i> ) (46)	SM12261_RS02220	97.2	HMPREF8579_1824	95.7	FD735_RS02200	97.0	SP_1853	97.5
	Galactose-1-phosphate uridylyltransferase 2 ( <i>galT2</i> ) (46)	SM12261_RS02225	94.9	HMPREF8579_1822	93.1	FD735_RS02210	92.3	SP_1852	96.2
Glc-DAG	Glycosyltransferase ( <i>spr0982</i> ) (47)	SM12261_RS04480	96.6	HMPREF8579_1104	88.4	FD735_RS04125	88.6	SP_1076	99.3
Gal-Glc-DAG	Glycosyltransferase ( <i>cpoA</i> ) (48)	SM12261_RS04475	97.4	HMPREF8579_1103	87.0	FD735_RS04120	87.3	SP_1075	99.7

<sup>a</sup>Abbreviations: UDP, uridine diphosphate; Glc, glucose (glucosyl); Gal, galactose (galactosyl); DAG, diacylglycerol.

<sup>b</sup>*S. pneumoniae* R6 gene was used as the reference.

<sup>c</sup>Percentage of amino acid sequence identity to the referenced enzyme.

SM43 *cdsA* and *pgsA* deletion mutants were analyzed. While the DHDAG glycolipid anchor (such as [M+Cl]<sup>-</sup> at *m/z* 953.6 of Fig. 2) is observed in the wild-type,  $\Delta$ *cdsA*, and  $\Delta$ *pgsA* strains, the Gro-P-linked DHDAG (such as [M-H]<sup>-</sup> at *m/z* 1071.6 of Fig. 2) is missing from the  $\Delta$ *cdsA* and  $\Delta$ *pgsA* strains. Identical anchor profiles were observed for the SM61 *cdsA* mutant (Table 1). These results demonstrate that *cdsA* and *pgsA*, or more specifically the ability to synthesize PG, are required for the biosynthesis of (Gro-P)-DHDAG in SM61 and SM43.

***S. mitis*, *S. oralis*, and *S. pneumoniae* cell extracts do not react with a type I LTA antibody.** Currently, enzymes known to transfer Gro-P from PG for Gro-P polymer synthesis or Gro-P modification include the following: (i) *S. aureus* LtaS, the type I LTA synthase that produces poly(Gro-P) (36); (ii) *L. monocytogenes* LtaP, the type I LTA primase that has an overall structure and active site sequences that are very similar to those of LtaS, except that it links only the first Gro-P unit to the glycolipid anchor (35, 40); and (iii) the recently identified streptococcal Gro-P transferase GacH that links Gro-P to cell wall-attached glycopolymers (50). Bioinformatic analyses predict no orthologs of either *ltaP* or *gacH* in the genomes of the mitis group streptococci assessed here, yet an ortholog of *ltaS* is present in *S. mitis* as previously reported (35).

If *S. mitis* *ltaS* functions the same as its ortholog in type I LTA-producing bacteria like *S. aureus*, polymers of Gro-P will be produced and may be detectable using an anti-type I LTA antibody. Western blot analysis using a previously described anti-type I LTA antibody was conducted for SM61, SM43, *S. oralis* ATCC 35037, and *S. pneumoniae* strains. No signal was detected from cell lysates of these strains (Fig. 3) or from cell lysates of SM61 that overexpress *ltaS* in *trans* from an anhydrotetracycline-inducible vector (Fig. S3). These results are in accordance with previous observations of no immunoluminescence detection of Gro-P polymers in SM61 (34). The validity of the antibody was confirmed by positive signals detected from cell lysates of *Streptococcus agalactiae*, *Streptococcus pyogenes*, and *S. aureus*, all three of which produce type I LTA (Fig. 3) (36, 51, 52). Interestingly, no signal was detected from cell lysate of *Enterococcus faecalis* OG1RF (Fig. 3), another bacterium known to produce type I LTA (53, 54), which as reported previously is poorly recognized by the anti-type I LTA antibody (55).

***S. mitis* LtaS mediates production of poly(Gro-P) in an *E. coli* heterologous host.** For the following analyses, the *S. mitis* type strain ATCC 49456 (SM61) was used as a model, and its *ltaS* ortholog (SM12261\_RS03435) was renamed *ltaS*. We heterologously expressed *S. mitis* *ltaS* in *E. coli* to verify the function of the gene. This approach was previously used in studies of *S. aureus* *ltaS* (36). Plasmid pET-*ltaS* (Table 3) was constructed so that the expression of *S. mitis* *ltaS* could be induced with isopropyl- $\beta$ -D-1-thiogalactopyranoside (IPTG) in *E. coli*. As shown in Fig. 4A, with the addition of IPTG,

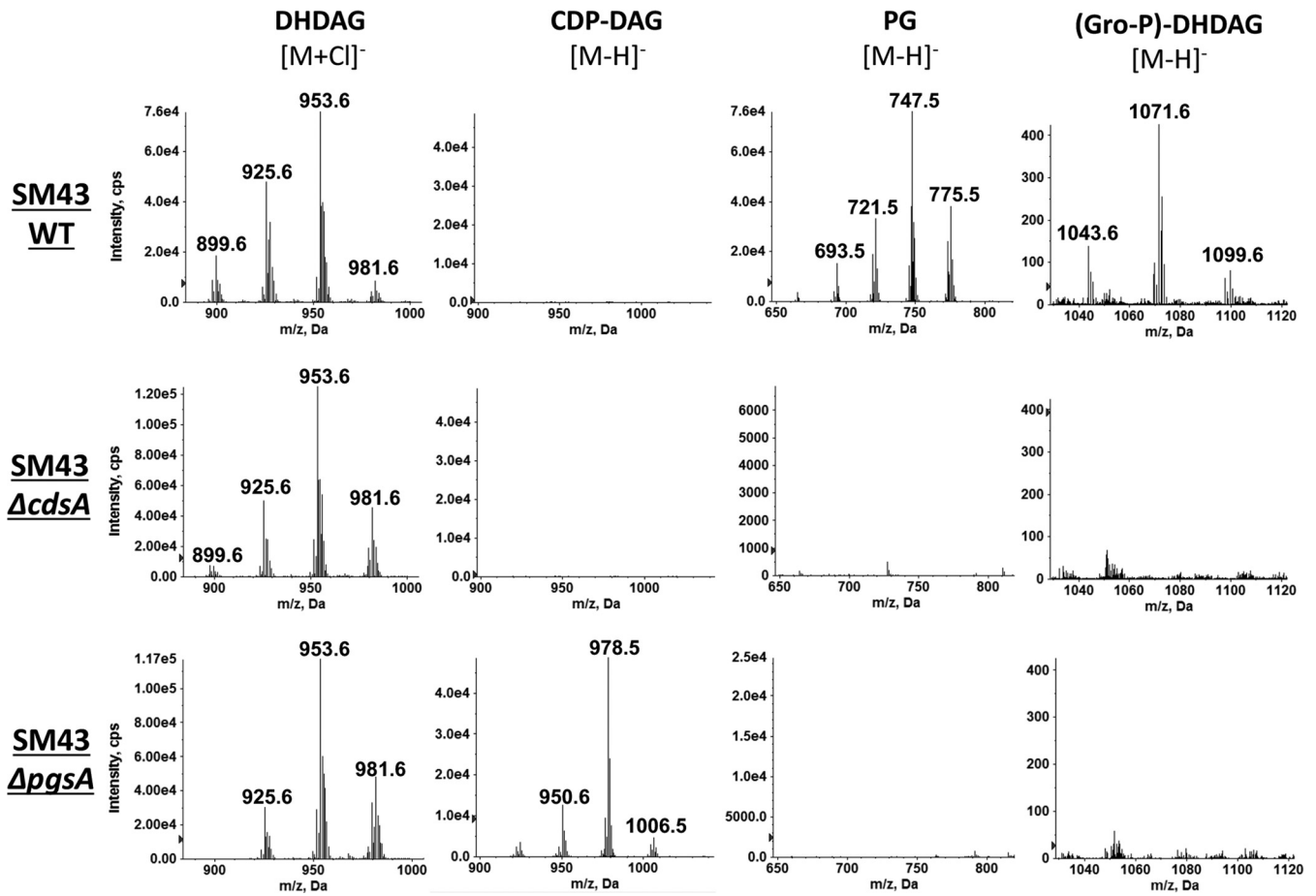


**FIG 2** Negative ion ESI mass spectra showing the detection of phospholipids and anchor profiles from lipid extracts of wild-type (WT) *Streptococcus* sp. 1643 (SM43) and  $\Delta cdsA$  and  $\Delta pgsA$  strains. Total lipids were extracted from SM43 cells grown to mid-log phase in Todd-Hewitt medium. From left to right, each column correspondingly shows the mass spectra of the  $[M+Cl]^-$  ions of dihexosyl-diacylglycerol (DHDAG) [retention time, ~8.0 to 10.0 min; most abundant  $m/z$  953.6 for DHDAG(16:0/18:1)],  $[M-H]^-$  ions of CDP-DAG [retention time, ~21.5 to 22.5 min; most abundant  $m/z$  978.5 for CDP-DAG(16:0/18:1)], phosphatidylglycerol (PG) [retention time, ~12.5 to 13.5 min; most abundant  $m/z$  747.5 for PG (16:0/18:1)], and glycerophosphate (Gro-P)-linked DHDAG [retention time, ~20.0 to 20.5 min; most abundant  $m/z$  1071.6 for (Gro-P)-DHDAG(16:0/18:1)]. The identification of these lipid species is supported by both exact mass measurement and MS/MS.

detectable bands produced by anti-type I LTA antibody targeting were observed for *E. coli* (pET-ltaS), demonstrating that *S. mitis ltaS* is sufficient to mediate the production of poly(Gro-P).

***S. mitis ltaS* complements an *S. aureus ltaS* mutant for type I LTA production.** In *S. aureus*, LtaS is required for proper cell division and efficient cell growth at 37°C (36,

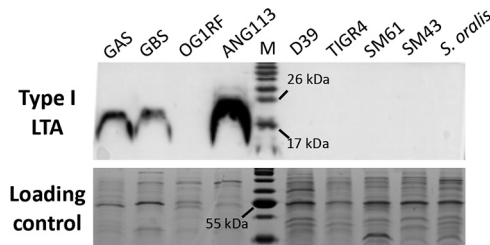


**FIG 3** Detection of type I LTA. Cell lysates from overnight cultures of *Streptococcus pyogenes* NZ131 (group A streptococci [GAS]), *S. agalactiae* A909 (group B streptococci [GBS]), *Enterococcus faecalis* OG1RF, *Staphylococcus aureus* (ANG113), *S. pneumoniae* D39, *S. pneumoniae* TIGR4, *S. mitis* ATCC 49456 (SM61), *Streptococcus* sp. 1643 (SM43), and *S. oralis* ATCC 35037 were analyzed. Lane M contains molecular mass standards (in kilodaltons). Anti-type I LTA antibody was used to detect the production of type I LTA. Loading control was stained with Coomassie blue.

**TABLE 3** Bacterial strains and plasmids used in this research

Species and strain or plasmid	Feature(s)	Reference or source
<i>Escherichia coli</i>		
DH5 $\alpha$	Cloning strain	73
K-12 MG1655	Model <i>E. coli</i> strain	74
BL21(DE3) pLys	Engineered <i>E. coli</i> strain for protein expression, contains Tn10 that produces T7 polymerase and plasmid pLys; the presence of pLys is maintained with 5 $\mu$ g/ml chloramphenicol	Novagen
<i>Streptococcus mitis</i>		
ATCC 49456 (SM61)	Type strain of <i>S. mitis</i>	ATCC
SM61 $\Delta$ <i>cdsA</i>	SM61 with coding region of <i>cdsA</i> (SM12261_RS08390) deleted	This study
SM61 $\Delta$ <i>ltaS</i>	SM61 with coding region of <i>ltaS</i> (SM12261_RS03435) replaced with gene <i>ermB</i>	This study
<i>Streptococcus</i> sp.		
1643 (SM43)	Mitis group <i>Streptococcus</i> isolated from infective endocarditis patient	42
SM43 $\Delta$ <i>cdsA</i>	SM43 with coding region of <i>cdsA</i> (FD735_RS08600) deleted	18
SM43 $\Delta$ <i>pgsA</i>	SM43 with coding region of <i>pgsA</i> (FD735_RS09695) replaced with gene <i>ermB</i>	18
<i>Streptococcus oralis</i>		
ATCC 35037	Type strain of <i>S. oralis</i>	ATCC
1647	Isolated from infective endocarditis patient	42
<i>Streptococcus pneumoniae</i>		
D39	Clinically isolated strain, serotype 2	75
TIGR4	Clinically isolated strain, serotype 4	76
<i>Streptococcus pyogenes</i>		
NZ131	Clinically isolated strain, serotype M49	ATCC
<i>Streptococcus agalactiae</i>		
A909	Isolated from a septic human neonate, serotype Ia	ATCC
<i>Staphylococcus aureus</i>		
ANG113	Strain RN4220, isogenic wild-type control of ANG499	36
ANG499	Generated from strain RN4220 (wild type), expression of chromosomal <i>ltaS</i> is induced with 1 mM IPTG; the genotype maintained with 5 $\mu$ g/ml erythromycin	36
<i>Enterococcus faecalis</i>		
OG1RF	Rifampin- and fusidic acid-resistant derivative of a human oral cavity isolate	77
Plasmids		
pABG5	Low-copy-number shuttle plasmid; confers kanamycin resistance	68
pitetR- <i>ltaS</i>	pABG5 with <i>S. mitis ltaS</i> coding region under control of tetracycline-inducible promoter P <sub><i>xyI/tet</i></sub>	This study
pitetR-SALtaS	pABG5 with <i>S. aureus ltaS</i> (SAV0719) coding region under control of promoter P <sub><i>xyI/tet</i></sub>	This study
pitetR	pitetR- <i>ltaS</i> that lacks the <i>ltaS</i> coding region and has EcoRI introduced; serves as empty plasmid control	This study
pET-28a(+)	Expression plasmid; confers kanamycin resistance	Novagen
pET- <i>ltaS</i>	pET-28a(+) with <i>S. mitis ltaS</i> under control of IPTG-inducible promoter	This study
pMSP3535	Confers erythromycin resistance; used to obtain <i>ermB</i> gene	7

56). To further confirm the physiological function of *S. mitis ltaS* in Gram-positive cells, we expressed it in a previously reported *S. aureus* strain that has its native *ltaS* gene under the control of an IPTG-inducible promoter (strain ANG499). Without IPTG, ANG499 is deficient for type I LTA production and has a growth defect when cultured at 37°C (36, 56). *S. mitis ltaS* was introduced into strain ANG499 by the plasmid pitetR-*ltaS* (Table 3), which has the *S. mitis ltaS* coding region under the control of the tetracycline-inducible promoter P<sub>*xyI/tet*</sub>. Addition of anhydrotetracycline (ATC) induces expression of *S. mitis ltaS*. Note that we included ATC in all experimental cultures described below, because we observed an ATC-dependent growth defect that confounded direct comparison of cultures grown in the presence or absence of ATC (Fig. S4).

As expected, strain ANG499 with the empty plasmid vector pitetR grew more slowly and reached a lower final optical density at 600 nm (OD<sub>600</sub>) value when cultured without IPTG compared to with IPTG (Fig. 4B). As expected, type I LTA production by *S. aureus ltaS* was induced by IPTG, confirmed by Western blot analysis (Fig. 4C) and detection of type I LTA intermediates (Gro-P)<sub>2</sub>-Glc<sub>2</sub>-DAG ([M-H]<sup>-</sup> ion at *m/z* 1214.6 of Fig. 5A) and alanine-linked (Gro-P)<sub>2</sub>-Glc<sub>2</sub>-DAG ([M-H]<sup>-</sup> ion at *m/z* 1285.7 of Fig. S5). Strikingly, the growth of ANG499 was also rescued by the expression of *S. mitis ltaS* from pitetR-*ltaS* (Fig. 4B), and type I LTA production was observed, as shown by Western blot

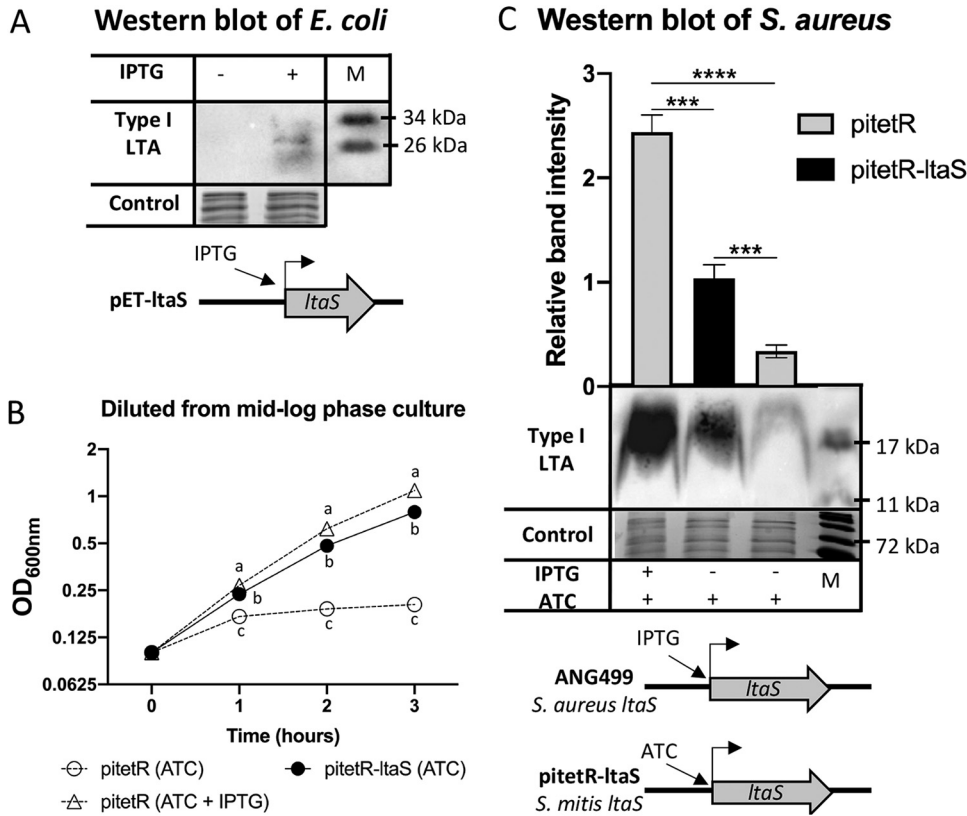


**FIG 4** Heterologous expression of *S. mitis ItaS* in *E. coli* and *S. aureus*. (A) Western blot detection of Gro-P polymers from *E. coli* containing plasmid pET-ItaS grown in liquid Luria-Bertani (LB) medium with the addition (+) of isopropyl- $\beta$ -D-1-thiogalactopyranoside (IPTG) and without (-) IPTG. IPTG was added to mid-log-phase bacterial cultures followed by another 30-min incubation at 37°C before cell pelleting. Three biological independent replicates were performed for each sample. (B) Growth curves of *S. aureus* ANG499 containing either pitetR or pitetR-ItaS grown in tryptic soy broth (TSB) with the addition of either 150 ng/ml anhydrotetracycline (ATC) only or 150 ng/ml ATC and 0.5 mM IPTG as indicated. Samples were grown in TSB with 0.5 mM IPTG overnight, followed by subculturing into fresh TSB with the indicated addition of induction reagents and incubated for 3 h. Then, another subculturing to an OD<sub>600</sub> of 0.1 with fresh media same as the previous incubation was performed. After the second subculture, OD<sub>600</sub> values were measured every hour and plotted. (C) Western blot detection of type I LTA from *S. aureus* ANG499 containing either pitetR or pitetR-ItaS. Samples were grown in the same way as described above for panel B, after the first subculturing and incubation, cells equal to 1 ml of OD<sub>600</sub> at 1.2 were harvested, followed by lysate preparation and immunodetection. Schematics of induction expression of chromosomal or plasmid-carried *ItaS* were shown in both panels A and C. Loading controls of both panels A and C were stained with Coomassie blue. Western blot band intensity in panel C was normalized to the loading control and the pitetR-ItaS sample. For panels B and C, four biological replicates were performed; averages of the sample values were plotted with the error bars depicting standard deviations. Statistical analyses were performed with one-way analysis of variance (ANOVA); significant difference was determined by  $P$  value of  $<0.05$ . For panel B, at a given time point, the a, b, and c letters each represent a statistical group that is significantly different from other groups;  $P$  values of all group comparisons are  $<10^{-6}$ . Statistical significance for panel C: \*\*\*,  $10^{-5} > P$  value  $> 10^{-6}$ ; \*\*\*\*,  $P$  value  $< 10^{-6}$ .

(Fig. 4C) and lipidomic analysis (Fig. 5A and Fig. S5). These data demonstrate that *S. mitis ItaS* can complement the function of *S. aureus ItaS* and promote production of type I LTA in *S. aureus*. Surprisingly, (Gro-P)-Glc<sub>2</sub>-DAG ([M-H]<sup>-</sup> ion at  $m/z$  1059.6 of Fig. 5B) was detected at comparable levels from all *S. aureus* cultures, including the native *ItaS*-deficient strain in the absence of IPTG induction.

**Expression of *S. aureus ItaS* does not confer detectable type I LTA signals in *S. mitis*.** To test whether *S. aureus ItaS* can mediate poly(Gro-P) production in *S. mitis*, *S. aureus ItaS* was introduced into *S. mitis* with the plasmid pitetR-SAltaS. Similar to pitetR-ItaS, pitetR-SAltaS encodes *S. aureus ItaS* under the control of the ATC-inducible promoter P<sub>xyI/tet</sub>. Type I LTA production was detected by Western blot analysis for *E. coli* (pitetR-SAltaS) induced with ATC (Fig. 6). However, no signals were observed for *S. mitis* (pitetR-SAltaS) induced with ATC. In addition, lipidomic analysis detected no further structure beyond a single Gro-P linked to DHDAG for *S. mitis* (pitetR-SAltaS) induced with ATC.

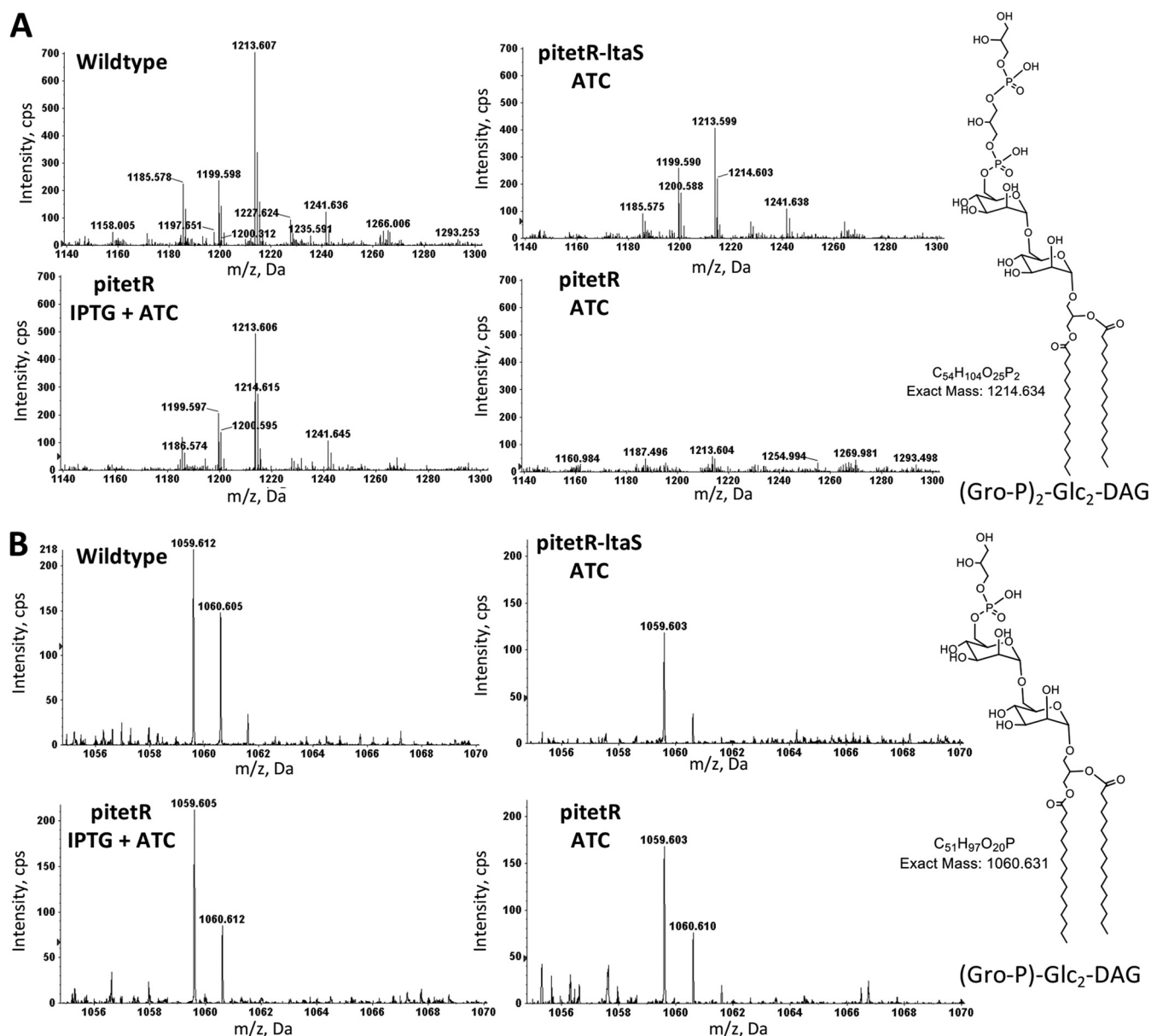


**FIG 5** MS detection of type I LTA biosynthetic precursors that contain one or two Gro-P units in the lipid extracts of *S. aureus*. *S. aureus* strain ANG113 (wild type), ANG499 containing plasmid pitetR-ItaS (pitetR-ItaS), and ANG499 containing the vector control pitetR (pitetR) were grown in liquid tryptic soy medium to late exponential phase with the addition of ATC and IPTG as indicated. Total lipids were extracted and analyzed with NPLC-ESI/MS in the negative ion mode. Shown are the mass spectra of the deprotonated  $[M-H]^-$  ions for (Gro-P)-Glc<sub>2</sub>-DAG (retention time, ~20.0 to 20.5 min; most abundant  $m/z$  1059.6) (A) and (Gro-P)<sub>2</sub>-Glc<sub>2</sub>-DAG (retention time, ~22.5 to 23.0 min; most abundant  $m/z$  1213.6) (B). The chemical structures presented are for illustrative purposes only. The stereochemistry and linkage of hexose moieties, as well as the phosphate position on the glycerol, could not be determined by tandem MS. Three biologically independent replicates were performed for each strain under each indicated culture condition. Abbreviations: Gro-P, glycerophosphate; Glc, glucosyl; DAG, diacylglycerol.

***S. mitis* lacking *ItaS* has increased serum susceptibility.** To investigate functions of *ItaS* in *S. mitis*, *ItaS* was deleted and exchanged for the erythromycin resistance marker *ermB*, generating *S. mitis*  $\Delta ItaS$ . Of note, (Gro-P)-DHDAG was still detected in the *S. mitis*  $\Delta ItaS$  strain, demonstrating that *ItaS* is not required for the addition of the Gro-P unit to the DHDAG (Table 1).

Unlike *S. aureus*, which requires *ItaS* for efficient growth, deletion of *ItaS* in *S. mitis* does not confer a growth defect under laboratory culturing conditions. Specifically, when growing in Todd-Hewitt broth at 37°C, the doubling time of the  $\Delta ItaS$  strain is 39.8 ( $\pm 3.7$ ) min, which is not significantly different from the 40.2 ( $\pm 3.5$ ) min doubling time of

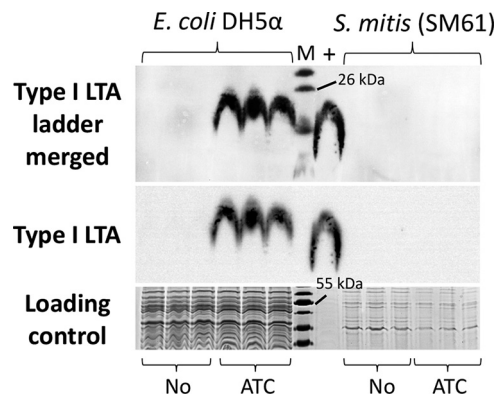


**FIG 6** Heterologous expression of *S. aureus ltaS* in *E. coli* and *S. mitis*. *E. coli* DH5 $\alpha$  and *S. mitis* ATCC 49456 (SM61) with pitetR-SAltaS were subcultured into media with no inducing agent (No) or with 150 ng/ml anhydrotetracycline (ATC). Cell lysate of *S. aureus* was used as a positive control (+). Western blot signal was obtained for 6-min cumulative exposure. The loading control was stained with Coomassie blue. Three biologically independent replicates are shown for each condition.

wild-type *S. mitis* (Fig. S6). Considering that the growth deficiency of *S. aureus* lacking *ltaS* could be mitigated by culturing at a lower temperature (56), the growth of wild-type *S. mitis* and  $\Delta ltaS$  strains cultured at a higher temperature was measured to determine whether the *ltaS* mutant was compromised for temperature-related stresses. The temperature 42°C was chosen as a representative of fever. Both wild-type and  $\Delta ltaS$  strains exhibited slower growth at 42°C compared to 37°C; however, no significant difference in growth rate was observed between the strains (46.2 [ $\pm 3.0$ ] and 47.4 [ $\pm 3.8$ ] min doubling times for the wild-type and  $\Delta ltaS$  strains, respectively). Moreover, no difference in susceptibilities to antibiotics targeting peptidoglycan biosynthesis, membrane integrity, and protein synthesis were observed (see Table S1 in the supplemental material). Thus, under these laboratory culture conditions, *ltaS* is not essential for the growth of *S. mitis*.

In addition, a potential role for *ltaS* in host-microbe interactions was investigated. As an oral commensal, the environment *S. mitis* colonizes is exposed to human gingival crevicular fluid, which is an extrudant of serum with lower concentrations of complement (57). Moreover, when invading the bloodstream and causing bacteremia and infectious endocarditis, *S. mitis* is constantly exposed to blood. Thus, human serum is a useful medium component for laboratory reconstruction of the host growth conditions. Supplementation of human serum into chemically defined medium (CDM) promotes the growth of *S. mitis* compared to nonsupplemented CDM (Fig. 7). Deletion of *ltaS* does not confer a significant difference in growth in Todd-Hewitt broth or unsupplemented CDM but does result in a significant growth deficiency in human serum-supplemented CDM, and makes *S. mitis* more sensitive to the killing effect of complete serum (Fig. 7). In addition, bacterial colony forming units (CFU)/ml counts were significantly higher for the  $\Delta ltaS$  mutant cultured in heat-inactivated serum compared to the mutant cultured in complete serum (Fig. 7); this significant difference was not observed for the wild-type strain. These results suggest that although *ltaS* is not required for growth of *S. mitis* under laboratory conditions, it confers protection against heat-sensitive serum components. Further investigation is needed to elucidate such interactions.

## DISCUSSION

In this work, we used NPLC-ESI/MS to analyze the glycolipid profiles of *S. mitis*, *S. oralis*, and *S. pneumoniae* strains. For all of the tested strains, biosynthetic intermediates of two structurally different LTAs were detected (Fig. 1 and Table 1). First, consistent with literature, the biosynthetic intermediates of the type IV LTA were detected, which is in agreement with genomic analysis of the biosynthetic genes (26). The

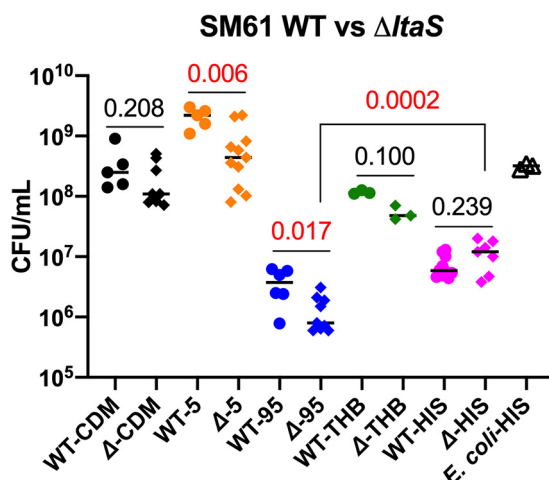


**FIG 7** Deletion of *ltaS* alters the responses of *S. mitis* ATCC 49456 (SM61) to human serum. Wild-type (WT) or  $\Delta$ *ltaS* SM61 ( $\Delta$ ) strains were cultured in chemically defined medium (CDM), CDM with 5% human serum (5), 95% human serum (95) with 5% phosphate-buffered saline (PBS), Todd-Hewitt broth (THB), and 95% heat-inactivated human serum (HIS) with 5% PBS. The CFU/ml of cultures after 8-h incubation are shown. The CFU/ml of *E. coli* K-12 MG1655 grown in 95% human serum is below the detection limit ( $10^5$ ; not shown in figure); the CFU/ml of *E. coli* cultured in HIS is shown. Each symbol represents the value for one biological independent repeat. Statistical analysis was performed with the Mann-Whitney method. *P* values are indicated above the line. Statistical significance was defined by *P* value of  $<0.05$ , and significant *P* values are shown in red.

second distinct LTA is indicated by the detection of (Gro-P)-DHDAG, which is similar to type I LTA polymers and unexpected based on previous reports, and thus has been the focus of this study.

On the basis of the results of genomic analysis, we proposed that the newly identified (Gro-P)-DHDAG is structured as (Gro-P)-Gal-Glc-DAG. The glycolipid Gal-Glc-DAG has been reported as the dominant glycolipid species in *S. pneumoniae*, and our prediction is in accordance with this previous report (43). However, the full pathway for Gal-Glc-DAG synthesis has not been fully experimentally verified in the mitis group streptococci; the stereochemistry of the hexoses requires further confirmation with structural analysis, such as with nuclear magnetic resonance (NMR).

The PG-dependent (Gro-P)-DHDAG biosynthetic process in *S. mitis* was then investigated, which led to the main focus of this study, functional verification of *S. mitis ltaS*. Through heterologous expression, we confirmed that *S. mitis ltaS* could directly synthesize Gro-P polymers in both *E. coli* and *S. aureus*. However, it appeared that *S. mitis ltaS* functions somewhat differently from *S. aureus ltaS*, as the expression of *S. mitis ltaS* does not fully complement the growth deficiency and the amount of type I LTA produced (Fig. 4B and C), which is not unexpected considering that *S. mitis* and *S. aureus ltaS* share only 38% sequence identity (26).

We did not detect a Gro-P polymer in wild-type *S. mitis* using Western blot analysis. Explanations as to why we could not detect the polymer include the following. (i) *S. mitis* does not produce the Gro-P polymer; instead, (Gro-P)-DHDAG is the complete and final product. (ii) A very small amount of the Gro-P polymer is produced under the culture conditions investigated here. (iii) Unique structural modifications on the Gro-P polymer hinder antibody recognition. (iv) *LtaS* acts on a different substrate than (Gro-P)-DHDAG in *S. mitis*. Further large-scale purification and structural analysis of the (Gro-P)-DHDAG-containing polymer produced by mitis group streptococci are required.

Interestingly, heterologous expression of *S. aureus ltaS* in *S. mitis* does not confer poly(Gro-P) production detectable by either Western blot or lipidomic analysis. It is possible that, as suggested above, unique structural modifications on the Gro-P polymer hinder antibody recognition or that *S. aureus ltaS* lacks the appropriate substrate

(s) in *S. mitis* to catalyze type I LTA synthesis, in which case further studies about the substrate recognition and binding activities of *S. aureus* and *S. mitis* LtaS are needed. Last but not the least, it is possible that the canonical LtaS enzymatic function of producing poly(Gro-P) is inhibited in *S. mitis*.

The findings that (Gro-P)-DHDAG is still present in *S. mitis*  $\Delta$ *ltaS*, as well as in *S. oralis* and *S. pneumoniae*, which are species that do not carry genes that encode any orthologs of *ltaS*, suggest the existence of an unknown PG-dependent Gro-P transferase in these species that is responsible for the synthesis of (Gro-P)-DHDAG. Unexpectedly, (Gro-P)-Glc<sub>2</sub>-DAG is also seen in *S. aureus* deficient for *ltaS*, suggesting that an unidentified Gro-P biosynthetic enzyme(s) or biological process(es) may exist in *S. aureus* as well, but this is more speculative.

In other Gram-positive pathogens that synthesize type I LTA, LtaS and its product, LTA, are essential for proper cell division (40, 56, 58, 59). Inhibiting the function of LtaS is effective in extending the survival of *S. aureus*-infected mice (60) and sensitizing multidrug-resistant *E. faecium* to antibiotics (61). Though *S. mitis* *ltaS* is not essential for proper growth of the bacterium in normal laboratory media or for synthesizing (Gro-P)-DHDAG, it does provide some advantage to *S. mitis* when human serum is present in the culture media and protects against the heat-sensitive serum components.

In summary, we provide evidence that a type I-like LTA might coexist with type IV LTA in *S. mitis*, *S. oralis*, and *S. pneumoniae* and queried the role of *ltaS* in this process in a model *S. mitis* strain. To our knowledge, there is only one previous report which documents a bacterial species producing two structurally different LTAs, in *Streptococcus suis*, an invasive pathogen of pigs (62). Our lipidomic and genomic studies show that we have an incomplete understanding of glycolipids, LTAs, and LtaS function in mitis group streptococci and their potential roles in host-microbe interactions.

## MATERIALS AND METHODS

**Bacterial strains and growth conditions.** Unless indicated otherwise, *E. coli* was grown in Luria-Bertani (LB) medium, *Streptococcus* strains were grown in Todd-Hewitt (TH) medium (BD Biosciences) with *S. pneumoniae* grown in TH medium supplemented with 0.5% yeast extract (BD Biosciences), and *E. faecalis* and *S. aureus* were grown in tryptic soy (TS) medium (BD Biosciences). All bacterial cultures were incubated at 37°C, unless otherwise noted. Streptococci were cultured with 5% CO<sub>2</sub>. Chemically defined medium (CDM) was made as previously described, with the addition of 0.5 mM choline (63). Human serum-supplemented medium was made by adding complete human serum (Sigma-Aldrich) to CDM to a final concentration of 5% (vol/vol). Antibiotic concentrations were as follows: kanamycin, 50 µg/ml in *E. coli*, 250 µg/ml in *S. aureus*, and 500 µg/ml in *S. mitis*; erythromycin, 50 µg/ml in *E. coli*. Transcription of genes controlled by the promoter P<sub>xyt/tet</sub> was induced with anhydrotetracycline (ATC) at a final concentration of 150 ng/ml. Isopropyl-β-D-1-thiogalactopyranoside (IPTG)-inducible expression was mediated by the addition of IPTG to a final concentration of 1 mM. Bacterial strains and plasmids used in this research are listed in Table 3.

**Sequence analysis.** Orthologs of glycolipid biosynthetic genes were identified through using the BLASTp function against the NCBI database (64). Specifically, genes of *S. pneumoniae* R6 (NCBI accession no. NC\_003098.1) were used as reference. The encoded amino acid sequences were input into BLASTp to search against the nonredundant protein database of *S. mitis* ATCC 49456 (taxid: 246201), *S. oralis* ATCC 35037 (taxid: 655813), *Streptococcus* sp. 1643 (taxid: 2576376), and *S. pneumoniae* TIGR4 (taxid: 170187) individually. The *ltaS* (SM12261\_RS03435) ortholog in *S. mitis* ATCC 49456 was identified similarly, with the amino acid sequence of *S. aureus* LtaS (SAV0719) (36) being the reference. Orthologs were determined by query coverage of >95% and E value of <10<sup>-120</sup>.

**Mutant generation.** Deletion of *cdsA* (SM12261\_RS08390) in *S. mitis* ATCC 49456 was conducted as previously described (65, 66). Briefly, approximately 2-kb flanking regions on either side of *cdsA* were amplified using Phusion polymerase (Thermo Fisher). PCR products were digested with restriction enzyme XmaI (New England Biolabs) and ligated with T4 DNA ligase (New England Biolabs). Ligated products were amplified using primers 61*cdsA*\_Up\_F and 61*cdsA*\_Dwn\_R (see Table S2 in the supplemental material), followed by gel extraction with the QIAquick gel extraction kit (Qiagen) per the manufacturer's instruction. The linear construct was transformed into *S. mitis* via natural transformation as described previously (66). The  $\Delta$ *cdsA* mutant was selected with 35 µg/ml daptomycin and confirmed by Sanger sequencing (Massachusetts General Hospital DNA Core) of the PCR product of the *cdsA* deletion region.

Deletion of *ltaS* in *S. mitis* ATCC 49456 was conducted similarly with some slight modifications. Specifically, a 1-kb DNA fragment containing *ermB* was generated through PCR amplification using plasmid pMSP3535 as the template (67). Then, splicing by overlap extension PCR was performed to produce a 5-kb amplicon that sequentially contained a 2-kb fragment upstream of *ltaS*, a 1-kb *ermB*-containing fragment in reverse orientation, and a 2-kb fragment downstream of *ltaS*. The PCR product was analyzed on a 0.8% agarose gel and extracted using the QIAquick gel extraction kit (Qiagen) per the

manufacturer's instruction. Transformation of the 5-kb amplicon into *S. mitis* was performed as described previously (66). The  $\Delta$ *ItaS* mutant was selected with 20  $\mu$ g/ml erythromycin and confirmed with Illumina genome sequencing (UTD Genome Core Facility).

**Plasmid construction.** Plasmids used in this research are listed in Table 3 with description of their functions. All primers used in this research are listed in Table S2.

The shuttle plasmid pABG5 was used for heterologous gene expression in Gram-positive bacteria (68). Specifically, the DNA fragment containing the *S. mitis* *ItaS* coding region was amplified using primers *LtaS\_F* and *LtaS\_R*, and the pABG5 plasmid backbone was linearized through PCR using primers pABG5-5 and pABG5-3. Gibson assembly was conducted per the manufacturer's instructions (NEBuilder HiFi DNA assembly master mix; New England Biolabs), followed by transformation of the product into *E. coli* DH5 $\alpha$ . The pABG5 with *ItaS* insert was further linearized with primers YW55 and YW56 and ligated with an 848-bp DNA fragment via Gibson assembly, producing the plasmid pitetR-*ItaS*. The 848-bp fragment contained a tetracycline-controlled promoter  $P_{xyI/tet}$  and the tetracycline repressor gene *tetR* in reverse orientation. Insertion of this 848-bp fragment immediately upstream of the *ItaS* coding region makes *ItaS* expression inducible by ATC addition. The sequence of the 848-bp fragment was obtained from plasmid pRMC2 in the Addgene sequence database (69, 70), and the fragment was synthesized commercially (Integrated DNA Technologies). Induced production of the target gene *ItaS* was confirmed by Western blotting. The empty vector control pitetR was constructed via linearization of pitetR-*ItaS* with PCR using primers YW58 and YW59, followed by Gibson assembly for gap closure. The removal of the *ItaS* coding region was confirmed by Sanger sequencing (Massachusetts General Hospital DNA Core). Plasmid pitetR has an EcoRI site inserted after the  $P_{xyI/tet}$ -controlled ribosomal binding site. ATC induction of *S. aureus* *ItaS* is mediated by plasmid pitetR-SAltaS. Specifically, an amplicon containing the *S. aureus* *ItaS* (SAV0719) coding region was obtained via PCR using primers YW72 and YW73, followed by Gibson assembly of this amplicon with linearized pitetR generated via EcoRI digestion. Successful insertion was confirmed with Sanger sequencing (Massachusetts General Hospital DNA Core), and the confirmed construct was transformed into *E. coli* DH5 $\alpha$  for expression analysis. Plasmid pET-*ItaS* that mediates isopropyl- $\beta$ -D-1-thiogalactopyranoside (IPTG)-inducible overexpression of *ItaS* was generated through insertion of the *ItaS* coding region immediately after the IPTG-inducible promoter region of pET-28a(+) (Novagen). Successful insertion was confirmed with Sanger sequencing (Massachusetts General Hospital DNA Core). The confirmed construct was transformed into *E. coli* BL21(DE3) pLys for expression analysis.

**Antibiotic susceptibility testing.** Antibiotic susceptibility testing was performed according to the bioMérieux Etest protocol with slight modifications. Specifically, a single colony of either the wild-type *S. mitis* ATCC 49456 or  $\Delta$ *ItaS* strain was selected from cation-adjusted Mueller-Hinton (MH) (BD Bacto) agar cultures, inoculated into 1 ml of MH broth, and incubated for 6 to 8 h at 37°C with 5% CO<sub>2</sub>. Then, 2 ml of fresh MH broth was added to the 1-ml culture, and incubation was resumed. After overnight incubation, the OD<sub>600</sub> of the cultures were measured, and samples having an OD<sub>600</sub> value of <0.2 were excluded from the following experimental procedures. Cultures were spread onto prewarmed MH agar plates with sterile cotton-tipped applicators, and plates were air dried for 15 to 20 min inside a biosafety cabinet. Then, Etest strips (Etest by bioMérieux) prewarmed to room temperature were applied to the plates with aseptic technique. The plates were incubated overnight at 37°C with 5% CO<sub>2</sub>. The MIC was determined by the intersection of the zone of inhibition with the Etest strip. At least three biological independent replicates were performed for each antibiotic-strain combination.

**Western blot analysis.** Detection of type I LTA via Western blot analysis was performed as previously described (39, 71).

For *E. coli*, single colonies were grown overnight in LB broth with appropriate antibiotics, followed by dilution to an OD<sub>600</sub> of 0.1 with fresh media into two replicates. For *E. coli* DH5 $\alpha$  containing pitetR-SAltaS, ATC was added to one set of cultures to a final concentration of 150 ng/ml, followed by 3-h incubation at 37°C before cell harvest. For *E. coli* BL21(DE3) pLys containing pET-*ItaS*, diluted bacterial cultures were incubated at 37°C for 3 h, and then IPTG was added to one set of cultures to a 1 mM final concentration, followed by another 30-min incubation at 37°C before cell harvest. To harvest cells, culture densities were normalized to an OD<sub>600</sub> of 0.6, and 1 ml was pelleted, washed, resuspended in 100  $\mu$ l of 2 $\times$  Laemmli sample buffer, and boiled for 15 min. Boiled samples were stored at -20°C prior to electrophoretic analysis.

For *S. aureus*, single colonies of each *S. aureus* strain were grown overnight in TS broth with 0.5 mM IPTG, 5  $\mu$ g/ml erythromycin, and 250  $\mu$ g/ml kanamycin, and then subcultured to an OD<sub>600</sub> of 0.1 into fresh TS broth containing 5  $\mu$ g/ml erythromycin, 250  $\mu$ g/ml kanamycin, and either 150 ng/ml ATC or 150 ng/ml ATC with 0.5 mM IPTG. After 3-h incubation, the OD<sub>600</sub> was measured, and cells equivalent to 1 ml of 1.2 OD<sub>600</sub> were pelleted. Cell pellets were washed and resuspended with 1 ml phosphate-buffered saline (PBS), followed by five cycles of bead-beating at 6.5 m/s for 45 s, with 5 min on ice between cycles (FastPrep-24; MP Biomedicals). After centrifugation at 200  $\times$  g for 1 min, cell lysates were collected, followed by pelleting at 17,000  $\times$  g for 10 min. The material was resuspended in 100  $\mu$ l of 2 $\times$  Laemmli sample buffer (Bio-Rad) followed by boiling for 15 min in a heating block.

For streptococci and *E. faecalis*, unless indicated, OD<sub>600</sub> values of the overnight cultures were measured, followed by pelleting of cells equivalent to 1 ml of 1.2 OD<sub>600</sub>. Induction of *ItaS* overexpression in *S. mitis* was conducted similarly as in *S. aureus*. Specifically, overnight cultures of *S. mitis* containing pitetR-*ItaS*, pitetR, or pitetR-SAltaS were diluted to an OD<sub>600</sub> value of 0.1 into fresh TH broth with 150 ng/ml ATC. After 7-h incubation, cells equivalent to 1 ml of a culture with an OD<sub>600</sub> of 1.2 were harvested. All cell pellets were washed and resuspended with 1 ml PBS, then followed with the same cell disruption and lysate preparation processes as described above for *S. aureus* samples.

Separation of cell lysate materials are conducted through sodium dodecyl sulfate-polyacrylamide gel electrophoresis (SDS-PAGE). Specifically, 15  $\mu$ l of each boiled sample was loaded onto a 15% SDS-

PAG gel, followed by electrophoresis at consistent 100 voltage and subsequent polyvinylidene difluoride (PVDF) membrane transfer at consistent 350 mA. The blocking solution was PBS containing 0.05% (wt/vol) Tween 20 and 10% (wt/vol) nonfat milk; antibody solutions were PBS with 0.05% (wt/vol) Tween 20 and 5% (wt/vol) nonfat milk. For *S. aureus* samples, 3  $\mu$ g/ml human IgG (Sigma) was added to the blocking and antibody solutions to block the activity of protein A. Primary antibody targeting type I LTA (clone 55; Hycult Technology) and secondary antibody (horseradish peroxidase [HRP]-conjugated anti-mouse IgG; Cell Signaling) were used at dilutions of 1:2,500 and 1:5,000, respectively. After adding HRP substrate (Immobilon Western; Millipore) and shaking at room temperature for 3 min, chemiluminescence signals were detected with the ChemiDoc touch imaging system (Bio-Rad) with default chemiluminescence settings. Relative band intensity was analyzed with the Image Lab Software (Bio-Rad).

**Lipidomic analysis.** Extraction of total lipids from stationary-phase cells was performed by acidic Bligh-Dyer extraction as previously described (18). Specifically, cells were grown to stationary phase in at least 5 ml of medium, followed by collection and storage at  $-80^{\circ}\text{C}$  until lipid extraction with the acidic Bligh-Dyer methods. The dried lipid extracts were dissolved in 100  $\mu$ l of chloroform-methanol (2:1, vol/vol). Typically, 10  $\mu$ l of the dissolved solution were injected for LC/MS analysis. NPLC-ESI/MS of lipids was performed as previously described (41, 72) using an Agilent 1200 quaternary LC system (Santa Clara, CA) coupled to a high-resolution TripleTOF5600 mass spectrometer (Sciex, Framingham, MA). An Ascentis Si high-performance liquid chromatography (HPLC) column (5  $\mu$ m; 25 cm  $\times$  2.1 mm; Sigma-Aldrich) was used. Mobile phase A consisted of chloroform-methanol-aqueous ammonium hydroxide (800:195:5, vol/vol/vol). Mobile phase B consisted of chloroform-methanol-water-aqueous ammonium hydroxide (600:340:50:5, vol/vol/vol/vol). Mobile phase C consisted of chloroform-methanol-water-aqueous ammonium hydroxide (450:450:95:5, vol/vol/vol/vol). The elution program was as follows: 100% mobile phase A was held isocratically for 2 min and then linearly increased to 100% mobile phase B for 14 min and held at 100% mobile phase B for 11 min. The LC gradient was then changed to 100% mobile phase C for 3 min and held at 100% mobile phase C for 3 min, and finally returned to 100% mobile phase A over 0.5 min and held at 100% mobile phase A for 5 min. Instrumental settings for negative ion ESI and MS/MS analysis of lipid species were as follows: ion spray voltage (IS) =  $-4,500$  V; current gas (CUR) = 20 lb/in<sup>2</sup> (pressure); gas-1 (GS1) = 20 lb/in<sup>2</sup>; declustering potential (DP) =  $-55$  V; and focusing potential (FP) =  $-150$  V. The MS/MS analysis used nitrogen as the collision gas. Data acquisition and analysis were performed using the Analyst TF1.5 software (Sciex, Framingham, MA).

**Serum survival test.** Overnight cultures of *S. mitis* were pelleted and washed with PBS, followed by subculturing into different media to an OD<sub>600</sub> of 0.1. Cultures were incubated at 37°C with 5% CO<sub>2</sub> for 8 h. At  $t=0$  and  $t=8$  h of incubation, bacterial CFU were quantified by serial dilution and plating on TH agar. *E. coli* K-12 MG1655 was prepared in a similar way described above and subcultured into 95% complete human serum (Sigma-Aldrich) and 95% heat-inactivated human serum to confirm the presence and absence of bactericidal activity, respectively. *E. coli* CFU were quantified by serial dilution and plating on LB agar.

## SUPPLEMENTAL MATERIAL

Supplemental material is available online only.

**FIG S1**, TIF file, 0.5 MB.

**FIG S2**, TIF file, 0.7 MB.

**FIG S3**, TIF file, 0.3 MB.

**FIG S4**, TIF file, 0.6 MB.

**FIG S5**, TIF file, 0.1 MB.

**FIG S6**, TIF file, 0.3 MB.

**TABLE S1**, PDF file, 0.1 MB.

**TABLE S2**, PDF file, 0.04 MB.

## ACKNOWLEDGMENTS

We gratefully acknowledge Angelika Grönding for providing the *S. aureus* strain ANG113 and ANG499.

This work was supported by grant R21AI130666 from the National Institutes of Health and the Cecil H. and Ida Green Chair in Systems Biology Science to K.L.P., grant R56AI139105 and R01AI148366 from the National Institutes of Health to K.L.P. and Z.G., and U54GM069338 to Z.G.

## REFERENCES

- Herrero ER, Slomka V, Bernaerts K, Boon N, Hernandez-Sanabria E, Passoni BB, Quirynen M, Teughels W. 2016. Antimicrobial effects of commensal oral species are regulated by environmental factors. *J Dent* 47:23–33. <https://doi.org/10.1016/j.jdent.2016.02.007>.
- Herrero ER, Slomka V, Boon N, Bernaerts K, Hernandez-Sanabria E, Quirynen M, Teughels W. 2016. Dysbiosis by neutralizing commensal mediated inhibition of pathobionts. *Sci Rep* 6:38179. <https://doi.org/10.1038/srep38179>.
- Thurnheer T, Belibasakis GN. 2018. *Streptococcus oralis* maintains homeostasis in oral biofilms by antagonizing the cariogenic pathogen *Streptococcus mutans*. *Mol Oral Microbiol* 33:234–239. <https://doi.org/10.1111/omi.12216>.

4. Wang B-Y, Kuramitsu HK. 2005. Interactions between oral bacteria: inhibition of *Streptococcus mutans* bacteriocin production by *Streptococcus gordonii*. *Appl Environ Microbiol* 71:354–362. <https://doi.org/10.1128/AEM.71.1.354-362.2005>.
5. Burne RA, Marquis RE. 2000. Alkali production by oral bacteria and protection against dental caries. *FEMS Microbiol Lett* 193:1–6. <https://doi.org/10.1111/j.1574-6968.2000.tb09393.x>.
6. Kim SL, Gordon SM, Shrestha NK. 2018. Distribution of streptococcal groups causing infective endocarditis: a descriptive study. *Diagn Microbiol Infect Dis* 91:269–272. <https://doi.org/10.1016/j.diagmicrobio.2018.02.015>.
7. Slipczuk L, Codolosa JN, Davila CD, Romero-Corral A, Yun J, Pressman GS, Figueredo VM. 2013. Infective endocarditis epidemiology over five decades: a systematic review. *PLoS One* 8:e82665. <https://doi.org/10.1371/journal.pone.0082665>.
8. Vincent LL, Otto CM. 2018. Infective endocarditis: update on epidemiology, outcomes, and management. *Curr Cardiol Rep* 20:86. <https://doi.org/10.1007/s11886-018-1043-2>.
9. Kilian M, Riley DR, Jensen A, Brüggemann H, Tettelin H. 2014. Parallel evolution of *Streptococcus pneumoniae* and *Streptococcus mitis* to pathogenic and mutualistic lifestyles. *mBio* 5:e01490-14. <https://doi.org/10.1128/mBio.01490-14>.
10. Kilian M, Poulsen K, Blomqvist T, Håvarstein LS, Bek-Thomsen M, Tettelin H, Sørensen UBS. 2008. Evolution of *Streptococcus pneumoniae* and its close commensal relatives. *PLoS One* 3:e2683. <https://doi.org/10.1371/journal.pone.0002683>.
11. Weiser JN, Ferreira DM, Paton JC. 2018. *Streptococcus pneumoniae*: transmission, colonization and invasion. *Nat Rev Microbiol* 16:355–367. <https://doi.org/10.1038/s41579-018-0001-8>.
12. O'Brien KL, Wolfson LJ, Watt JP, Henkle E, Deloria-Knoll M, McCall N, Lee E, Mulholland K, Levine OS, Cherian T, Hib and Pneumococcal Global Burden of Disease Study Team. 2009. Burden of disease caused by *Streptococcus pneumoniae* in children younger than 5 years: global estimates. *Lancet* 374:893–902. [https://doi.org/10.1016/S0140-6736\(09\)61204-6](https://doi.org/10.1016/S0140-6736(09)61204-6).
13. Kawamura Y, Hou XG, Sultana F, Miura H, Ezaki T. 1995. Determination of 16S rRNA sequences of *Streptococcus mitis* and *Streptococcus gordonii* and phylogenetic relationships among members of the genus *Streptococcus*. *Int J Syst Bacteriol* 45:406–408. <https://doi.org/10.1099/00207713-45-2-406>.
14. Dowson CG, Coffey TJ, Kell C, Whiley RA. 1993. Evolution of penicillin resistance in *Streptococcus pneumoniae*; the role of *Streptococcus mitis* in the formation of a low affinity PBP2B in *S. pneumoniae*. *Mol Microbiol* 9:635–643. <https://doi.org/10.1111/j.1365-2958.1993.tb01723.x>.
15. Pimenta F, Gertz RE, Park SH, Kim E, Moura I, Milucky J, Roupheal N, Farley MM, Harrison LH, Bennett NM, Bigogo G, Feikin DR, Breiman R, Lessa FC, Whitney CG, Rajam G, Schiffer J, Da Gloria Carvalho M, Beall B. 2018. *Streptococcus infantis*, *Streptococcus mitis*, and *Streptococcus oralis* strains with highly similar *cps5* loci and antigenic relatedness to serotype 5 pneumococci. *Front Microbiol* 9:3199. <https://doi.org/10.3389/fmicb.2018.03199>.
16. Shekhar S, Khan R, Schenck K, Petersen FC. 2019. Intranasal immunization with the commensal *Streptococcus mitis* confers protective immunity against pneumococcal lung infection. *Appl Environ Microbiol* 85:e02235-18. <https://doi.org/10.1128/AEM.02235-18>.
17. Law SH, Chan ML, Marathe GK, Parveen F, Chen CH, Ke LY. 2019. An updated review of lysophosphatidylcholine metabolism in human diseases. *Int J Mol Sci* 20:1149. <https://doi.org/10.3390/ijms20051149>.
18. Joyce LR, Guan Z, Palmer KL. 2019. Phosphatidylcholine biosynthesis in mitis group streptococci via host metabolite scavenging. *J Bacteriol* 201:e00495-19. <https://doi.org/10.1128/JB.00495-19>.
19. Baddiley J. 1972. Teichoic acids in cell walls and membranes of bacteria. *Essays Biochem* 8:35–77.
20. Ryu YH, Baik JE, Yang JS, Kang SS, Im J, Yun CH, Kim DW, Lee K, Chung DK, Ju HR, Han SH. 2009. Differential immunostimulatory effects of Gram-positive bacteria due to their lipoteichoic acids. *Int Immunopharmacol* 9:127–133. <https://doi.org/10.1016/j.intimp.2008.10.014>.
21. Jeong JH, Jang S, Jung BJ, Jang KS, Kim BG, Chung DK, Kim H. 2015. Differential immune-stimulatory effects of LTAs from different lactic acid bacteria via MAPK signaling pathway in RAW 264.7 cells. *Immunobiology* 220:460–466. <https://doi.org/10.1016/j.imbio.2014.11.002>.
22. Han SH, Kim JH, Martin M, Michalek SM, Nahm MH. 2003. Pneumococcal lipoteichoic acid (LTA) is not as potent as staphylococcal LTA in stimulating Toll-like receptor 2. *Infect Immun* 71:5541–5548. <https://doi.org/10.1128/iai.71.10.5541-5548.2003>.
23. Percy MG, Gründling A. 2014. Lipoteichoic acid synthesis and function in Gram-positive bacteria. *Annu Rev Microbiol* 68:81–100. <https://doi.org/10.1146/annurev-micro-091213-112949>.
24. Goebel WF, Shedlovsky T, Lavin GI, Adams MH. 1943. The heterophile antigen of pneumococcus. *J Biol Chem* 148:1–15. [https://doi.org/10.1016/S0021-9258\(18\)72310-7](https://doi.org/10.1016/S0021-9258(18)72310-7).
25. Gisch N, Kohler T, Ulmer AJ, Mühling J, Pribyl T, Fischer K, Lindner B, Hammerschmidt S, Zähringer U. 2013. Structural reevaluation of *Streptococcus pneumoniae* lipoteichoic acid and new insights into its immunostimulatory potency. *J Biol Chem* 288:15654–15667. <https://doi.org/10.1074/jbc.M112.446963>.
26. Denapaite D, Brückner R, Hakenbeck R, Vollmer W. 2012. Biosynthesis of teichoic acids in *Streptococcus pneumoniae* and closely related species: lessons from genomes. *Microb Drug Resist* 18:344–358. <https://doi.org/10.1089/mdr.2012.0026>.
27. Kilian M, Tettelin H. 2019. Identification of virulence-associated properties by comparative genome analysis of *Streptococcus pneumoniae*, *S. pseudopneumoniae*, *S. mitis*, three *S. oralis* subspecies, and *S. infantis*. *mBio* 10:e01985-19. <https://doi.org/10.1128/mBio.01985-19>.
28. Gisch N, Schwudke D, Thomsen S, Heß N, Hakenbeck R, Denapaite D. 2015. Lipoteichoic acid of *Streptococcus oralis* Uo5: a novel biochemical structure comprising an unusual phosphorylcholine substitution pattern compared to *Streptococcus pneumoniae*. *Sci Rep* 5:16718. <https://doi.org/10.1038/srep16718>.
29. Bergström N, Jansson PE, Kilian M, Skov Sørensen UB. 2000. Structures of two cell wall-associated polysaccharides of a *Streptococcus mitis* biovar 1 strain: a unique teichoic acid-like polysaccharide and the group O antigen which is a C-polysaccharide in common with pneumococci. *Eur J Biochem* 267:7147–7157. <https://doi.org/10.1046/j.1432-1327.2000.01821.x>.
30. Bergström N, Jansson PE, Kilian M, Skov Sørensen UB. 2003. A unique variant of streptococcal group O-antigen (C-polysaccharide) that lacks phosphocholine. *Eur J Biochem* 270:2157–2162. <https://doi.org/10.1046/j.1432-1033.2003.03569.x>.
31. Rosan B. 1978. Absence of glycerol teichoic acids in certain oral streptococci. *Science* 201:918–920. <https://doi.org/10.1126/science.684416>.
32. Hamada S, Mizuno J, Kotani S, Torii M. 1980. Distribution of lipoteichoic acids and other amphipathic antigens in oral streptococci. *FEMS Microbiol Lett* 8:93–96. <https://doi.org/10.1111/j.1574-6968.1980.tb05057.x>.
33. Ohkuni H, Todome Y, Mizuse M, Ohtani N, Suzuki H, Igarashi H, Hashimoto Y, Ezaki T, Harada K, Imada Y, Ohkawa S, Kotani S. 1993. Biologically active extracellular products of oral viridans streptococci and the aetiology of Kawasaki disease. *J Med Microbiol* 39:352–362. <https://doi.org/10.1099/00222615-39-5-352>.
34. Hogg SD, Whiley RA, De Soet JJ. 1997. Occurrence of lipoteichoic acid in oral streptococci. *Int J Syst Bacteriol* 47:62–66. <https://doi.org/10.1099/00207713-47-1-62>.
35. Campeotto I, Percy MG, MacDonald JT, Förster A, Freemont PS, Gründling A. 2014. Structural and mechanistic insight into the *Listeria monocytogenes* two-enzyme lipoteichoic acid synthesis system. *J Biol Chem* 289:28054–28069. <https://doi.org/10.1074/jbc.M114.590570>.
36. Gründling A, Schneewind O. 2007. Synthesis of glycerol phosphate lipoteichoic acid in *Staphylococcus aureus*. *Proc Natl Acad Sci U S A* 104:8478–8483. <https://doi.org/10.1073/pnas.0701821104>.
37. Karatsa-Dodgson M, Wörmann ME, Gründling A. 2010. *In vitro* analysis of the *Staphylococcus aureus* lipoteichoic acid synthase enzyme using fluorescently labeled lipids. *J Bacteriol* 192:5341–5349. <https://doi.org/10.1128/JB.00453-10>.
38. Reichmann NT, Gründling A. 2011. Location, synthesis and function of glycolipids and polyglycerolphosphate lipoteichoic acid in Gram-positive bacteria of the phylum *Firmicutes*. *FEMS Microbiol Lett* 319:97–105. <https://doi.org/10.1111/j.1574-6968.2011.02260.x>.
39. Gründling A, Schneewind O. 2007. Genes required for glycolipid synthesis and lipoteichoic acid anchoring in *Staphylococcus aureus*. *J Bacteriol* 189:2521–2530. <https://doi.org/10.1128/JB.01683-06>.
40. Webb AJ, Karatsa-Dodgson M, Gründling A. 2009. Two-enzyme systems for glycolipid and polyglycerolphosphate lipoteichoic acid synthesis in *Listeria monocytogenes*. *Mol Microbiol* 74:299–314. <https://doi.org/10.1111/j.1365-2958.2009.06829.x>.
41. Adams HM, Joyce LR, Guan Z, Akins RL, Palmer KL. 2017. *Streptococcus mitis* and *S. oralis* lack a requirement for CdsA, the enzyme required for synthesis of major membrane phospholipids in bacteria. *Antimicrob Agents Chemother* 61:e02552-16. <https://doi.org/10.1128/AAC.02552-16>.
42. Akins RL, Katz BD, Monahan C, Alexander D. 2015. Characterization of high-level daptomycin resistance in viridans group streptococci developed upon

- in vitro exposure to daptomycin. *Antimicrob Agents Chemother* 59:2102–2112. <https://doi.org/10.1128/AAC.04219-14>.
43. Brundish DE, Shaw N, Baddiley J. 1965. The glycolipids from the non-capsulated strain of *Pneumococcus* I-192R, A.T.C.C. 12213. *Biochem J* 97:158–165. <https://doi.org/10.1042/bj0970158>.
  44. Mollerach M, López R, García E. 1998. Characterization of the *galU* gene of *Streptococcus pneumoniae* encoding a uridine diphosphoglucose pyrophosphorylase: a gene essential for capsular polysaccharide biosynthesis. *J Exp Med* 188:2047–2056. <https://doi.org/10.1084/jem.188.11.2047>.
  45. Holden HM, Rayment I, Thoden JB. 2003. Structure and function of enzymes of the Leloir pathway for galactose metabolism. *J Biol Chem* 278:43885–43888. <https://doi.org/10.1074/jbc.R300025200>.
  46. Ayoola MB, Shack LA, Nakama MF, Thornton JA, Swiatlo E, Nanduri B. 2019. Polyamine synthesis effects capsule expression by reduction of precursors in *Streptococcus pneumoniae*. *Front Microbiol* 10:1996. <https://doi.org/10.3389/fmicb.2019.01996>.
  47. Berg S, Edman M, Li L, Wikström M, Wieslander Å. 2001. Sequence properties of the 1,2-diacylglycerol 3-glucosyltransferase from *Acholeplasma laidlawii* membranes. Recognition of a large group of lipid glycosyltransferases in eubacteria and archaea. *J Biol Chem* 276:22056–22063. <https://doi.org/10.1074/jbc.M102576200>.
  48. Edman M, Berg S, Storm P, Wikström M, Vikström S, Öhman A, Wieslander Å. 2003. Structural features of glycosyltransferases synthesizing major bilayer and nonbilayer-prone membrane lipids in *Acholeplasma laidlawii* and *Streptococcus pneumoniae*. *J Biol Chem* 278:8420–8428. <https://doi.org/10.1074/jbc.M211492200>.
  49. Lanie JA, Ng WL, Kazmierczak KM, Andrzejewski TM, Davidsen TM, Wayne KJ, Tettelin H, Glass JI, Winkler ME. 2007. Genome sequence of Avery's virulent serotype 2 strain D39 of *Streptococcus pneumoniae* and comparison with that of unencapsulated laboratory strain R6. *J Bacteriol* 189:38–51. <https://doi.org/10.1128/JB.01148-06>.
  50. Edgar RJ, van Hensbergen VP, Ruda A, Turner AG, Deng P, Le Breton Y, El-Sayed NM, Belew AT, McIver KS, McEwan AG, Morris AJ, Lambeau G, Walker MJ, Rush JS, Korotkov KV, Widmalm G, van Sorge NM, Korotkova N. 2019. Discovery of glycerol phosphate modification on streptococcal rhamnose polysaccharides. *Nat Chem Biol* 15:463–471. <https://doi.org/10.1038/s41589-019-0251-4>.
  51. Fischer W, Koch HU, Rösel P, Fiedler F, Schmuck L. 1980. Structural requirements of lipoteichoic acid carrier for recognition by the poly(ribitol phosphate) polymerase from *Staphylococcus aureus* H. A study of various lipoteichoic acids, derivatives, and related compounds. *J Biol Chem* 255:4550–4556. [https://doi.org/10.1016/S0021-9258\(19\)85528-X](https://doi.org/10.1016/S0021-9258(19)85528-X).
  52. Henneke P, Morath S, Uematsu S, Weichert S, Pfitzenmaier M, Takeuchi O, Müller A, Poyart C, Akira S, Berner R, Teti G, Geyer A, Hartung T, Trieu-Cuot P, Kasper DL, Golenbock DT. 2005. Role of lipoteichoic acid in the phagocyte response to Group B *Streptococcus*. *J Immunol* 174:6449–6455. <https://doi.org/10.4049/jimmunol.174.10.6449>.
  53. Theilacker C, Kaczynski Z, Kropiec A, Fabretti F, Sange T, Holst O, Huebner J. 2006. Opsonic antibodies to *Enterococcus faecalis* strain 12030 are directed against lipoteichoic acid. *Infect Immun* 74:5703–5712. <https://doi.org/10.1128/IAI.00570-06>.
  54. Huebner J, Quaes A, Krueger WA, Goldmann DA, Pier GB. 2000. Prophylactic and therapeutic efficacy of antibodies to a capsular polysaccharide shared among vancomycin-sensitive and -resistant enterococci. *Infect Immun* 68:4631–4636. <https://doi.org/10.1128/iai.68.8.4631-4636.2000>.
  55. Baik JE. 2015. Molecular structure and immunological function of lipoteichoic acid purified from *Enterococcus faecalis*. PhD thesis. Seoul National University, Seoul, South Korea.
  56. Oku Y, Kurokawa K, Matsuo M, Yamada S, Lee B-L, Sekimizu K. 2009. Pleiotropic roles of polyglycerolphosphate synthase of lipoteichoic acid in growth of *Staphylococcus aureus* cells. *J Bacteriol* 191:141–151. <https://doi.org/10.1128/JB.01221-08>.
  57. Lamster IB. 1997. Evaluation of components of gingival crevicular fluid as diagnostic tests. *Ann Periodontol* 2:123–137. <https://doi.org/10.1902/annals.1997.2.1.123>.
  58. Schirmer K, Marles-Wright J, Lewis RJ, Errington J. 2009. Distinct and essential morphogenic functions for wall- and lipo-teichoic acids in *Bacillus subtilis*. *EMBO J* 28:830–842. <https://doi.org/10.1038/emboj.2009.25>.
  59. Garufi G, Hendrickx AP, Beeri K, Kern JW, Sharma A, Richter SG, Schneewind O, Missiakas D. 2012. Synthesis of lipoteichoic acids in *Bacillus anthracis*. *J Bacteriol* 194:4312–4321. <https://doi.org/10.1128/JB.00626-12>.
  60. Richter SG, Elli D, Kim HK, Hendrickx APA, Sorg JA, Schneewind O, Missiakas D. 2013. Small molecule inhibitor of lipoteichoic acid synthesis is an antibiotic for Gram-positive bacteria. *Proc Natl Acad Sci U S A* 110:3531–3536. <https://doi.org/10.1073/pnas.1217337110>.
  61. Paganelli FL, van de Kamer T, Brouwer EC, Leavis HL, Woodford N, Bonten MJM, Willems RJL, Hendrickx APA. 2017. Lipoteichoic acid synthesis inhibition in combination with antibiotics abrogates growth of multidrug-resistant *Enterococcus faecium*. *Int J Antimicrob Agents* 49:355–363. <https://doi.org/10.1016/j.ijantimicag.2016.12.002>.
  62. Gisch N, Auger JP, Thomsen S, Roy D, Xu J, Schwudke D, Gottschalk M. 2018. Structural analysis and immunostimulatory potency of lipoteichoic acids isolated from three *Streptococcus suis* serotype 2 strains. *J Biol Chem* 293:12011–12025. <https://doi.org/10.1074/jbc.RA118.002174>.
  63. Van De Rijn I, Kessler RE. 1980. Growth characteristics of group A streptococci in a new chemically defined medium. *Infect Immun* 27:444–448. <https://doi.org/10.1128/IAI.27.4.444-448.1980>.
  64. Altschul SF, Madden TL, Schäffer AA, Zhang J, Zhang Z, Miller W, Lipman DJ. 1997. Gapped BLAST and PSI-BLAST: a new generation of protein database search programs. *Nucleic Acids Res* 25:3389–3402. <https://doi.org/10.1093/nar/25.17.3389>.
  65. Morrison DA, Khan R, Junges R, Åmdal HA, Petersen FC. 2015. Genome editing by natural genetic transformation in *Streptococcus mutans*. *J Microbiol Methods* 119:134–141. <https://doi.org/10.1016/j.mimet.2015.09.023>.
  66. Salvadori G, Junges R, Morrison DA, Petersen FC. 2016. Overcoming the barrier of low efficiency during genetic transformation of *Streptococcus mitis*. *Front Microbiol* 7:1009. <https://doi.org/10.3389/fmicb.2016.01009>.
  67. Bryan EM, Bae T, Kleerebezem M, Dunny GM. 2000. Improved vectors for nisin-controlled expression in Gram-positive bacteria. *Plasmid* 44:183–190. <https://doi.org/10.1006/plas.2000.1484>.
  68. Granok AB, Parsonage D, Ross RP, Caparon MG. 2000. The RofA binding site in *Streptococcus pyogenes* is utilized in multiple transcriptional pathways. *J Bacteriol* 182:1529–1540. <https://doi.org/10.1128/jb.182.6.1529-1540.2000>.
  69. Geissendörfer M, Hillen W. 1990. Regulated expression of heterologous genes in *Bacillus subtilis* using the Tn10 encoded *tet* regulatory elements. *Appl Microbiol Biotechnol* 33:657–663. <https://doi.org/10.1007/BF00604933>.
  70. Corrigan RM, Foster TJ. 2009. An improved tetracycline-inducible expression vector for *Staphylococcus aureus*. *Plasmid* 61:126–129. <https://doi.org/10.1016/j.plasmid.2008.10.001>.
  71. Wei Y, Kouse AB, Murphy ER. 2017. Transcriptional and posttranscriptional regulation of *Shigella shuT* in response to host-associated iron availability and temperature. *Microbiol Open* 6:e442. <https://doi.org/10.1002/mbo3.442>.
  72. Tan BK, Bogdanov M, Zhao J, Dowhan W, Raetz CRH, Guan Z. 2012. Discovery of a cardiolipin synthase utilizing phosphatidylethanolamine and phosphatidylglycerol as substrates. *Proc Natl Acad Sci U S A* 109:16504–16509. <https://doi.org/10.1073/pnas.1212797109>.
  73. Taylor RG, Walker DC, McInnes RR. 1993. *E. coli* host strains significantly affect the quality of small scale plasmid DNA preparations used for sequencing. *Nucleic Acids Res* 21:1677–1678. <https://doi.org/10.1093/nar/21.7.1677>.
  74. Jensen KF. 1993. The *Escherichia coli* K-12 “wild types” W3110 and MG1655 have an *rph* frameshift mutation that leads to pyrimidine starvation due to low *pyrE* expression levels. *J Bacteriol* 175:3401–3407. <https://doi.org/10.1128/jb.175.11.3401-3407.1993>.
  75. Slager J, Aprianto R, Veening JW. 2018. Deep genome annotation of the opportunistic human pathogen *Streptococcus pneumoniae* D39. *Nucleic Acids Res* 46:9971–9989. <https://doi.org/10.1093/nar/gky725>.
  76. Tettelin H, Nelson KE, Paulsen IT, Eisen JA, Read TD, Peterson S, Heidelberg J, DeBoy RT, Haft DH, Dodson RJ, Durkin AS, Gwinn M, Kolonay JF, Nelson WC, Peterson JD, Umayam LA, White O, Salzberg SL, Lewis MR, Radune D, Holtzapple E, Khouri H, Wolf AM, Utterback TR, Hansen CL, McDonald LA, Feldblyum TV, Angiuoli S, Dickinson T, Hickey EK, Holt IE, Loftus BJ, Yang F, Smith HO, Venter JC, Dougherty BA, Morrison DA, Hollingshead SK, Fraser CM. 2001. Complete genome sequence of a virulent isolate of *Streptococcus pneumoniae*. *Science* 293:498–506. <https://doi.org/10.1126/science.1061217>.
  77. Gold OG, Jordan HV, van Houte J. 1975. The prevalence of enterococci in the human mouth and their pathogenicity in animal models. *Arch Oral Biol* 20:473–477. [https://doi.org/10.1016/0003-9969\(75\)90236-8](https://doi.org/10.1016/0003-9969(75)90236-8).